Stark broadening of high principal quantum number hydrogen Balmer lines in low-density laboratory plasmas

E. Stambulchik
Weizmann Institute of Science, Rehovot 76100, Israel

S. Alexiou
University of Crete, TETY, 71409 Heraklion, TK2208, Greece

H. R. Griem and P. C. Kepple
Institute for Research in Electronics and Applied Physics, University of Maryland, College Park, Maryland 20742, USA

(Received 18 October 2006; published 3 January 2007; publisher error corrected 17 January 2007)

We present results for Stark broadening of high principal quantum number (up to $n=15$) Balmer lines, using an analytical (the "standard theory") approach and two independently developed computer simulation methods. The line shapes are calculated for several sets of plasma parameters, applicable to radio-frequency discharge ($N_e \approx 10^{13}$ cm^{-3}) and magnetic fusion ($N_e \approx 10^{15}$ cm^{-3}) experiments. Comparisons of the calculated line profiles to the experimental data show a very good agreement. Density and temperature dependences of the linewidths, as well as relative contributions of different Stark-broadening mechanisms, are analyzed. It is seen that the standard theory of line broadening is sufficiently accurate for the entire set of plasma conditions and spectral transitions considered here, while an alternative theory ("advanced generalized theory") is shown to be inadequate for the higher-density region. A discussion of possible reasons for this disagreement is given.

DOI: 10.1103/PhysRevE.75.016401 PACS number(s): 52.55.Fa, 32.70.Jz, 52.80.Pi, 32.60.+i

I. INTRODUCTION

Early members of the Lyman, Balmer, and Paschen series of hydrogen are usually broadened mostly by Doppler, Zeeman, and opacity effects at electron densities below, say, $N_e \approx 10^{15}$ cm^{-3}. However, Stark broadening caused by ion- and electron-produced electric fields tends to dominate over Doppler broadening for lines from upper levels with principal quantum numbers $n \gtrsim 10$ in plasmas with electron densities down to $N_e \approx 10^{13}$ cm^{-3} (assuming the kinetic temperature is well below 1 eV). If a reliable theory of this Stark broadening were available, the measurement of the widths or profiles of these lines would provide an electron density diagnostic, e.g., for tokamak edge plasmas [1–3] and other magnetic fusion energy (MFE) experiments [4]. For an independent verification of the theory, separate accurate experiments supported, e.g., by interferometric electron density measurements, are most desirable, like those in radio-frequency discharges (RFDs) [5,6].

Since densities and temperatures in the latter experiments are lower than those in the MFE experiments by factors of about 40 and 30, respectively, future verification experiments also for the conditions in MFE devices are definitely needed to assess the validity of any theory. Lacking such sufficiently accurate experiments, one must reconsider the validity of the approximations underlying the theories used for the Stark broadening calculations. This will be attempted in the following section for the two theories employed so far, namely, the "standard theory" (ST) [7–9] and the "advanced generalized theory" (AGT) [10,11].

Lately, several computer simulation methods (CSMs) have been developed addressing the needs to cover plasma conditions where analytical calculations are not feasible (e.g., see [12,13]). Thus far, however, simulations have been mostly restricted to rather low-lying Lyman, Balmer, and Paschen lines. To the best of our knowledge, no CSM results for transitions involving atomic levels with principal quantum number (PQN) as high as 15 have appeared in the literature. In the third section, accurate numerical simulations will be presented and corrections to the basic quasistatic [14] and impact [15] approximations used in ST will then be estimated.

II. VALIDITY OF THE BASIC APPROXIMATIONS

Corrections to these basic approximations might have been anticipated by applying the validity criterion for the quasistatic approximation, namely, that Stark shifts caused by an ion be larger than the inverse duration of the corresponding ion-atom collision. Since in the AGT paper [16] concerning the lines and plasma conditions of interest here, analytical expressions [17] for the wings of hydrogen (and one-electron ion) lines were used, it is appropriate to invoke Eq. (48) of [17] for these critical Stark shifts, i.e., in our case

$$\Delta\omega_{c,i} = \frac{4kTm_e}{3\hbar(n_u^2 - n_\ell^2)m_p^*}. \tag{1}$$

Here, n_u and n_ℓ are upper- and lower-state principal quantum numbers, and m_e and m_p^* are the mass of electrons and reduced (in the center-of-gravity frame of radiator and perturber) mass of the perturbing ions. Converting from angular frequencies to wavelengths (in Å), one thus finds

$$\Delta\lambda_{c,i} = \frac{\gamma}{n_u^2 - 12 + 48/n_u^2 - 64/n_u^4} \tag{2}$$

for Balmer lines in $kT=0.15$-eV hydrogen and 5-eV deuterium plasmas, where $\gamma=0.234$ and 3.89, respectively. These

shifts turn out to be smaller by factors $\gtrsim 13$ or 33 than the observed half width at half maximum (HWHM) linewidths in Refs. [5,6] and [1–3], respectively. This leaves only a very small wavelength range containing the central dips of lines without unshifted Stark components, and the rather weak unshifted Stark components, susceptible to any significant ion-dynamical corrections to ST calculations. (Strictly speaking, these estimates are of course not valid for lines with strong unshifted components, e.g., not for H-alpha, nor should they be interpreted too rigorously in view of the averages over several parameters involved and the overlap of different collisions.)

The criterion just discussed can be applied to the electron collisions as well. Namely, Stark shifts smaller than the inverse of the duration of a typical electron-atom collision would then indicate the validity of the impact approximation. To test for this, one may use Eq. (1) letting $m_p = m_e$, i.e., without the m_e/m_p^* factor. Corresponding $\Delta\lambda_{c,e}$ values are larger than the measured half widths by factors $\gtrsim 15$ for all lines in the tokamak experiments [1–3], but, e.g., only by factors of about 4 and 1.5 for the $n=12$ line in [5] and the $n=15$ line in Ref. [6], respectively. For the other lines in these radio-frequency discharges, one finds larger factors, up to 73 for $n=6$. However, for the $n \gtrsim 12$ lines, the validity of the electron impact approximation clearly needs to be checked, although corresponding errors in HWHM widths may be surprisingly small. As was first recognized by Kogan [18], (suitably improved) impact and quasistatic approximations yield rather similar linewidths in this transition regime. This is in part because the total fields from overlapping collisions are actually smoother in their time dependence than assumed in the usual impact-approximation calculations (see also [9]). One should also keep in mind that for the lines and parameter range in question, strong collisions usually constitute a non-negligible part of the total impact width; and therefore standard perturbative impact calculations may carry corresponding error bars (typically $\leqslant 10\%$). The simulations described in the next section are free from these issues.

III. NUMERICAL SIMULATIONS

In this paper, we present results of nonperturbative CSM calculations utilizing two independent implementations. The first calculation approach uses the collision-time statistics method [19–21] and is described in Ref. [22]; in addition, optimization techniques [23,24] were applied, resulting in significant speedup factors (up to ≈ 40 for the $n=15$ Balmer line).[1] The second approach is described in Ref. [25]. Further on, these two calculational methods will be referred to as CSM1 and CSM2, respectively.

In all calculations, the following assumptions were made: (i) Only the dipole interaction $V=-\vec{D}\cdot\vec{E}$ is taken into account when evaluating perturbations due to the plasma fields. (Here, $\vec{D}$ is the dipole operator and $\vec{E}$ is the perturbing field.) (ii) Interactions between states with different principal quantum numbers (PQNs) are neglected. (iii) Only dipole transitions are considered for the line-shape calculation. The validity of these assumptions, as well as corresponding uncertainties in the results, will be discussed later on.

There are a few principal differences between the CSM1 and CSM2 methods, as applied in the present calculations. Both methods used the quasiparticle model (Debye-shielded perturbers moving along straight path trajectories), which is fully justified for such weakly coupled plasmas as considered here. However, in the CSM1 simulations the Debye screening of all quasiparticles was assumed to be due to electrons only, whereas in CSM2 for each sort of quasiparticles the Debye length was assigned differently [25], e.g., the protons in the RFD case were assumed to be screened by both electrons and protons themselves. (Different types of *Ansätze* approximating true microfields via the quasiparticle microfields have been suggested and used in other calculations, see, e.g., [26]. However, as will be shown below, the collective effects play only a minor role for the plasmas considered.) Also, CSM2 uses the particle re-injection at the boundary of the simulation volume, while for CSM1 the use of the collision-time statistics method [19–21] ensures that less than one particle in 1000 is missed by the simulation and no re-injection is required. The difference between CSM1 and CSM2 in the assumed Debye potentials for ion perturbers makes a rather minor difference in the linewidths for weakly coupled plasmas. Indeed, the Debye electric field $F=e(1+\xi)\exp(-\xi)/r^2$, where $\xi \equiv r/\rho_D$, can be expanded for $\xi \ll 1$ as $F \approx e(1-\xi^2/2)/r^2$. Therefore a relative change in the electric field due to $\rho_D \rightarrow \rho_D/\sqrt{2}$ is $\xi^2/2$. Using for r a typical ion-ion separation $r_{ii}=(\frac{4\pi}{3}N_e)^{-1/3}$, the relative difference in the ion-induced linewidths between the two methods can be estimated as

$$\Delta_{CSM1,CSM2} \approx \frac{3}{2}\Gamma, \tag{3}$$

where Γ is the plasma coupling parameter.

Another difference is in the way the spectrum $L(\omega)$ is calculated. CSM1 (and several other Stark-broadening simulation methods) proceeds with taking the Fourier transform of the dipole-correlation function $\mathrm{Tr}\vec{D}(0)\cdot\vec{D}(t)$. However, CSM2 skips the calculation of $C(t)$ altogether and instead evaluates $|\vec{D}(\omega)|^2$, where $\vec{D}(t)$ is the dipole operator and $\vec{D}(\omega)$ is its Fourier transform (here, we omit numerical factors irrelevant for the comparison). In both cases, the procedure is repeated many times and averaged, which corresponds to an averaging over a statistically representative ensemble of radiators. For the purpose of comparison we substitute $|\vec{D}(\omega)|^2$ with $\int dt \exp(-i\omega t)\int_0^{t_{max}} d\tau \vec{D}(\tau)\cdot\vec{D}(t+\tau)$. Then, the two approaches can be formally described in a unified way:

$$L(\omega) = \frac{1}{\pi}\,\mathrm{Re}\int_0^{t_{max}} dt \exp(-i\omega t)\langle C(t)\rangle_{N_r}, \tag{4}$$

where $\langle\ \rangle_{N_r}$ denotes an average over the number of runs N_r, each done for the time t_{max}, and

[1] We note that, within the limits of validity of the assumptions described below, these optimizations involve no approximation.

$$C(t) = \begin{cases} \mathrm{Tr}\vec{D}(0)\cdot\vec{D}(t) & \text{in CSM1}, \\ t_{max}^{-1}\mathrm{Tr}\int_0^{t_{max}} d\tau \vec{D}(\tau)\cdot\vec{D}(t+\tau) & \text{in CSM2}. \end{cases}$$

Therefore the difference comes down to whether the full autocorrelation function of $\vec{D}(t)$ is used (CSM2) or a single term of it (CSM1). However, since $C(t)$ is always averaged over an ensemble of radiators, the two approaches are equivalent as long as the ergodic theorem holds, i.e., averages over an ensemble and over time are the same. (However, N_r required to achieve a given finite accuracy is, in general, different for CSM1 and CSM2.) Evidently, this is true for the stationary plasmas modeled in the present work. More generally, the requirement is for the plasma parameters to change negligibly during the typical correlation time $t_c \sim \mathrm{HWHM}^{-1}$ of a given transition.

The spin-orbit effects were taken into account only approximately for most of the CSM2 calculations by assigning to an nl state the energy equal to a weighted average of energies of its fine-structure components. (Further on, this will be referred to as a "residual LS" approximation.) However, in a few cases where the spin-orbit interactions are non-negligible, the line shapes were calculated with the spin degree of freedom taken into account accurately. In the CSM1 calculations presented here, fine-structure effects were neglected.

The accuracy of the calculations is discussed in the Appendix.

IV. RESULTS

By and large, among the experimental works on high-n transitions in hydrogen, only the data from the RFD measurements [5,6] can be considered as a reference. Furthermore, the low plasma density in the RFD conditions (1.2×10^{13} cm^{-3}) made the set of physical assumptions implied by the simulations, in particular neglecting higher-than-dipole multipole interactions, fully justified. (The quadrupole interactions contribute less than 1% to the linewidths, as is indicated by comparison of our ST calculations with and without the quadrupole corrections.) Table I lists our calculated FWHM widths for the H_6–H_{12} and H_{15} lines (the Balmer transitions originating from upper levels with PQN of 6–12 and 15, respectively). We note that the fine-structure effect is not completely negligible for the lower-n part of Balmer transitions covered in the present study; in particular, as seen from Table I, for the H_6 and H_7 transitions this amounts to about 10% and 5%, respectively. For higher n, the relative contribution of the spin-orbit interaction becomes smaller, e.g., of the order of 1% for $n=10$. A minor systematic difference between the CSM1 and CSM2 values is believed to be due to the different approach to the ion Debye screening, and is consistent with the simple estimate [see Eq. (3)] which gives about 5% for this difference. For higher PQN the difference should be smaller, as the relative importance of electrons in the broadening becomes larger. It should be noted, however, that the differences between the CSM1 and CSM2 results do not exceed the combined error bars.

TABLE I. FWHM (Å) of high-n H Balmer transitions in RFD plasma ($N_e=1.2\times10^{13}$ cm^{-3}, $T=0.16$ eV).

Line	ST	CSM1	CSM2
H_6	0.190	0.181	0.194[a]
H_7	0.233	0.259	0.259[a]
H_8	0.364	0.360	0.334
H_9	0.449	0.458	0.434
H_{10}	0.591	0.572	0.549
H_{11}	0.723	0.735	0.683
H_{12}	0.877	0.906	0.834
H_{15}	1.38	1.39	1.37

[a]Calculated with the fine-structure effect taken into account rigorously. The H_6 and H_7 FWHM values obtained using the "residual LS" approximation (see the text) are 0.180 and 0.249 Å, respectively. In the pure-degenerate case (to be compared to the other results in the same rows), the widths are 0.174 and 0.245 Å, respectively.

In Table II we compare our results with the experimental data [5,6]. The agreement is very good, taking into account the quoted 10% accuracy in the experimental determination of the electron density and a possible slight inhomogeneity of the plasma [5]. We note that the use of an effective 2350-K temperature to account for both the real temperature (1850 K) and the magnetic-field-induced broadening in Ref. [5] was an overestimate, in our opinion. To check for the importance of the magnetic field, we performed a calculation of the H_6 line broadening with the 1200-G magnetic field taken into account rigorously, using the CSM2 method. The difference in the linewidth was found to be below 1%. For higher-n transitions, the effect of the magnetic field should be even smaller. Therefore when performing the convolution of the calculated spectra with the Doppler broadening, the 1850-K Gaussians were used. In the table, we also quote the AGT results, to be discussed below. Figures 1 and 2 present our calculated and experimental [27] profiles of the RFD H_9 and H_{10} transitions, respectively. The calculated profiles include the Doppler broadening (which is rather minor for

TABLE II. Ratios of the experimental FWHM widths [6] to our calculated widths from Table I after convolution with the 0.16-eV Doppler broadening. For discussion, the AGT results from Ref. [6] are quoted as well.

Line	ST	CSM1	CSM2	AGT[a]
H_6	0.92	0.97	0.93	0.94/0.87
H_7	0.91	0.95	0.93	0.94/0.84
H_8	0.94	0.95	0.99	1.07/0.94
H_9	0.91	0.89	0.97	0.99/0.87
H_{10}	0.92	0.97	0.99	1.11/0.96
H_{11}	0.91	0.88	0.96	1.01/0.89
H_{12}	0.89	0.87	0.93	1.05/0.91
H_{15}	0.96	0.96	0.97	1.02/0.92

[a]Values with and without "dynamical intensities" correction. (See also Sec. V.)

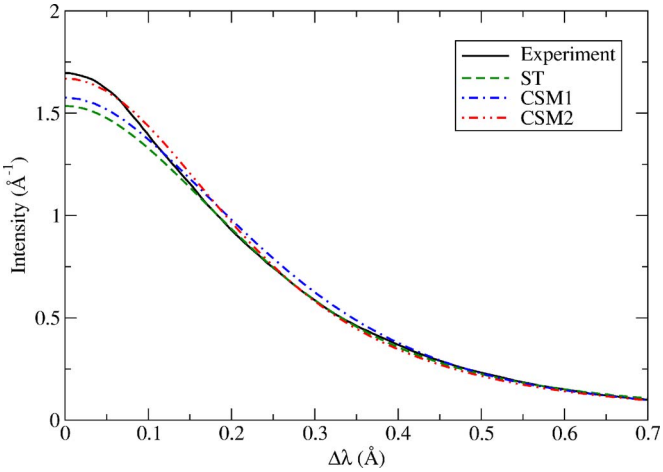

FIG. 1. (Color online) Comparison of the calculated and measured [27] H_9 profiles. $N_e=1.2\times10^{13}$ cm^{-3}, $T=0.16$ eV. The calculated profiles are given after the convolution with the Doppler broadening. All profiles are area normalized.

these two lines, contributing only $\lesssim$10% and $\lesssim$5% for H_9 and H_{10}, respectively). These figures demonstrate a very good agreement between the different calculations and the measured data over the entire line profiles, not only the FWHM values. (The slightly steeper decay of the measured profiles is possibly due to the plasma inhomogeneity.)

Also, we present results for typical plasma conditions found in the MFE experiments. For these conditions, there is a rather significant spread between the ST and AGT results. For example, based on the Stark widths of the $n=8$, 9, 10, and 11 Balmer transitions, quoted in Ref. [1] to be 4.7, 5.9, 7.5, and 9.6 Å, respectively, the electron density was estimated to be $(5.4\pm0.2)\times10^{14}$ cm^{-3} (the best fit values varied from line to line within the error bars mentioned), whereas AGT infers N_e as high as 6.6×10^{14} cm^{-3} [16]. In addition, the experimental conditions of Ref. [1] (such as a non-negligible instrumental broadening, presence of impurity lines in the spectra, and a rather strong magnetic field) do not

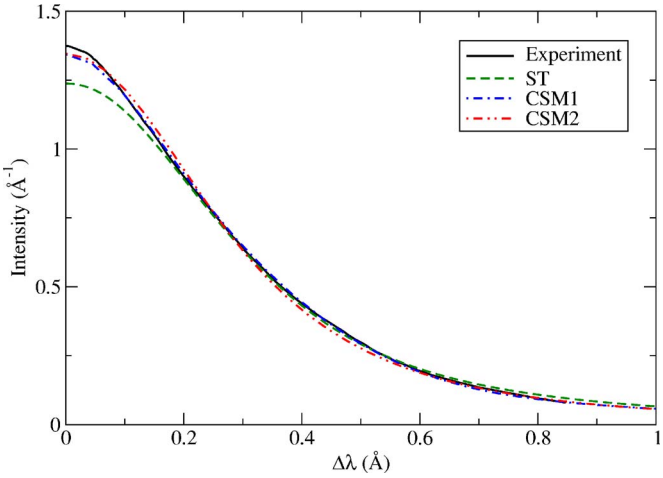

FIG. 2. (Color online) Comparison of the calculated and measured [27] H_{10} profiles. $N_e=1.2\times10^{13}$ cm^{-3}, $T=0.16$ eV. The calculated profiles are given after the convolution with the Doppler broadening. All profiles are area normalized.

TABLE III. FWHM (Å) of high-nD Balmer transitions for typical MFE conditions ($N_e=5.0\times10^{14}$ cm^{-3}, $T=4$ eV).

Line	ST[a]	CSM1	CSM2
D_6	2.60/2.48	2.64	2.49
D_7	3.20/2.88	3.53	3.37
D_8	4.93/4.70	4.42	4.54
D_9	6.17/5.74	5.96	5.80
D_{10}	8.14/7.73	7.66	7.34
D_{11}	9.90/9.22	9.60	9.13

[a]Values with and without quadrupole corrections.

allow, in our opinion, for the determination of the N_e value with a higher than, say, 10% accuracy, no matter how accurate the Stark broadening calculations might be. Therefore it is not our intent here to fit the available high-n MFE experimental data. Instead, we shall choose an arbitrary set of plasma parameters ($N_e=5.0\times10^{14}$ cm^{-3}, $T=4$ eV) which is not far from either of the existing results, and then investigate the N_e and T dependences of the high-n Stark broadening, both in the proximity of this set of parameters and in a rather broad range, covering the entire region between the RFD and MFE plasma conditions.

The MFE calculation results are listed in Table III. With respect to the ST results quoted in the table, these were obtained with and without quadrupole interactions between ions and atoms. In Table IV we compare the ST, AGT, and simulation results for another set of plasma parameters, namely those inferred from AGT in Ref. [16]. In this comparison the ST values quoted are without the effects of quadrupole interactions and inelastic collisions, i.e., the same as in AGT and the simulations. As seen from this table, the AGT results are smaller than the CSM values by 15–20 %, whereas the ST widths match the computer simulations better, exceeding them by 5–10 % only.

V. DISCUSSION

Before checking the accuracy of ST calculations [7,9] for the two plasma conditions by our numerical simulations discussed in the previous sections, some remarks need to be made on the AGT calculations [10,11,16], besides referring the interested reader to discussions of various shortcomings of this theory summarized by some of us and Halenka and

TABLE IV. Comparison of FWHM results for the MFE conditions assumed in Ref. [16] ($N_e=6.6\times10^{14}$ cm^{-3}, $T=7.7$ eV).

Line	AGT	ST	CSM1	CSM2
D_8	4.7[a]	6.0	5.66	5.46
D_9	5.9	7.4	7.15	7.06
D_{10}	7.5	9.9	9.45	8.88
D_{11}	9.6	12.0	11.5	11.0

[a]In Ref. [16], this value is quoted as 4.9 Å, which appears to be a typographical error.

Olchawa in two recent papers [28,29]. According to Ref. [16] "impact ions" dominate for the lines of interest here because of the "collapse" [30] of the splitting of Stark components due to nonadiabatic collisions (which are, of course, allowed for in the ST calculations), although a correction for quasistatic splitting is finally made in Eq. (10) of [16] according to the asymptotic (wing) formulas of Stehle [17]. The corresponding effective damping constants are, however, not directly related to the half widths, since the various profile contributions are not all Lorentzians. This oversimplification and the overestimate of the ion broadening by strong ion collisions due to the neglect of Kogan's smoothing [18] may well have led to the errors in the AGT calculations indicated by our numerical simulations. We also note that, in contrast to the statements made in Ref. [31], the AGT shortcomings are *not* addressed by "latest developments" [32] in AGT. AGT remains basically a unified version of an impact-based theory, i.e., it is still manifestly binary. As a result, the ion dynamics, in the case of essentially overlapping ion collisions, cannot be treated correctly. (We note that the ion dynamics effects are taken into account naturally in our CSM calculations, and appear to have very little impact on the linewidths considered here, as is discussed below.)

To assess the importance in ST of electrons, ions, and unitarity-violating strong electron collisions, we present in Table V relative contributions of the above quoted ST FWHMs. Specifically, we quote the ion quasistatic width (QS), the pure electron width (E), and the contribution of weak electron collisions only (W). (The ion QS widths of transitions with a central unshifted component are not listed, since for such transitions FWHM is zero in the nonquenching quasistatic limit. Also, because the QS line shapes are not Lorentzian, the QS and E values in each row do not necessarily add up to 100% exactly.) These results confirm that for the parameters in question, the ionic contribution is always more than half the width. The effect of cutoffs is quite minor, as evidenced by rather close values of E and W in each case. In addition, by comparing the ST results with the penetrating ST calculations [33], we verified that the penetrating collisions are not important here ($\lesssim 1\%$).

According to Table II, the FWHM linewidths from our simulations agree very well with the experimental data, as do both ST and AGT. The latter, however, purports to refine itself by the invocation of so-called "dynamical intensities" [6]. We note that the experimental conditions for which the dynamical intensities (in the original sense, as defined in Ref. [34]) should be used, imply that the emission takes place essentially in a vacuum, so that the electron and, especially, the ion collisional processes are too weak to compete with the radiative decay rate. This is evidently not the case for the RFD plasma as can be extrapolated from Table 3 in Ref. [35] for $n=3$, 4, and 5. More direct estimates of the critical proton densities for statistical populations at $kT=1$ eV can be obtained from Fig. 4 of Ref. [36], namely about 3×10^{7} cm^{-3} for $n=6$ and down to 10^{4} cm^{-3} for $n=15$. Furthermore, the collisional rates grow with PQN, while, at the same time, the radiative rates drop considerably. Therefore even assuming that these corrections can be noticeable at all, one would expect them to decrease sharply for higher-n transitions. On the contrary, the AGT "dynamical intensities" corrections appear to be practically constant for all transitions considered, from H_6 to H_{15}. However, given an entire absence of any mathematical formulary supporting the claims made in Ref. [6], we shall refrain from further analysis. Suffice it to note also that (i) the experimental accuracy in the determination of the plasma density was 10%, (ii) the fine splitting effects, found to contribute, e.g., about 10% to the H_6 linewidth for the plasma considered, were omitted, and (iii) the issue of the Doppler broadening is not mentioned in Ref. [6] at all, probably meaning either the use of the overestimated effective temperature as in the original Ref. [5] or an omission of the Doppler convolution. Each of the above sources of inaccuracies might be responsible for a-few-percent differences in the resulting widths. Having this in mind, the marginally better agreement with the experimental data due to the questionable dynamical intensities correction should be considered as purely coincidental. On the other hand, our computer simulations achieve a very good agreement with the experimental data without any such additions.

TABLE V. Comparison of relative ST FWHM's (%) of high-n H or D Balmer transitions for the typical RFD ($N_e=1.2\times10^{13}$ cm^{-3}, $T=0.16$ eV) and MFE ($N_e=5.0\times10^{14}$ cm^{-3}, $T=4$ eV) plasma conditions.

	RFD			MFE		
Line	QS	E	W	QS	E	W
H_6	70	26	24	74	22	20
H_7		34	31		31	28
H_8	63	34	31	65	32	30
H_9		40	36		38	35
H_{10}	56	44	37	58	43	38
H_{11}		48	41		46	42
H_{12}	55	51	43			
H_{15}		57	47			

While in the RFD case there are, within the associated inaccuracies, no principal differences in the results produced by ST, AGT, and the computer simulations, in the case of the higher-density MFE plasmas the situation is quite different. As follows from Tables III and IV, ST and the two CSM approaches remain in a reasonable agreement between themselves, whereas AGT produces significantly different results (Table IV). To the best of our knowledge, the only systematic experimental study of high-n Balmer transitions in the plasma conditions similar to MFE was performed using an afterglow of a large-Z discharge [37]. In this work, an agreement with ST calculations within the experimental error bars was recorded. However, the sum of the experimental uncertainties (due to the density determination, shot-to-shot reproducibility, and a presence of unexplained asymmetries in the individual line profiles) is, in our opinion, too high to allow an ultimate check of the Stark-broadening calculations.

We point out that, in the absence of independent accurate measurements of the plasma parameters in Refs. [1–4], a mere agreement with the experimental linewidths cannot be considered as a sign of validity of any given theory or calculation. Instead, it is customary (and instructive) to look at the N_e dependence of the Stark broadening. Therefore we

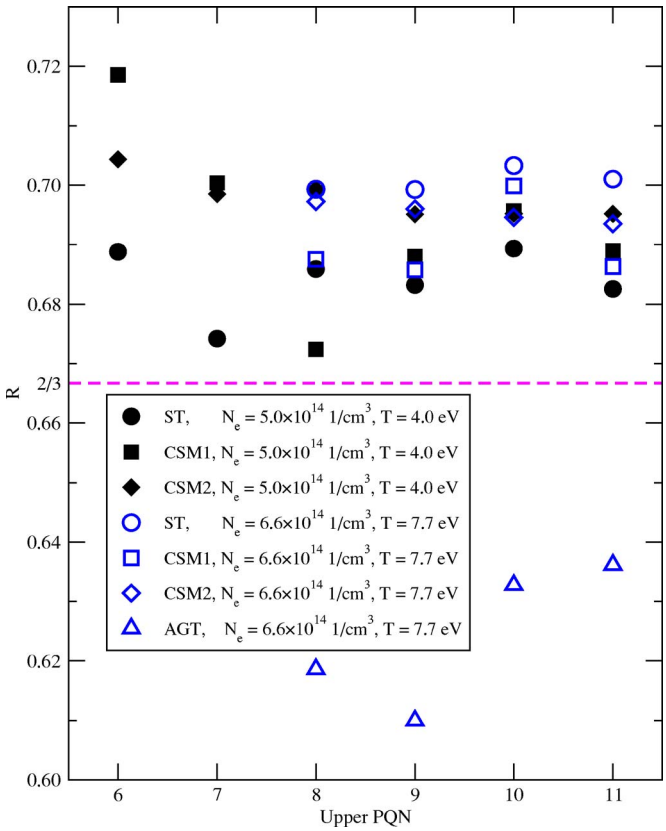

FIG. 3. (Color online) The R ratio, as defined by Eq. (6). The AGT data are taken from Refs. [6,16]. The RFD plasma parameters are as in Table I, and MFE plasma parameters are indicated in the legend.

proceed by comparing the MFE results to the corresponding RFD ones. Indeed, in spite of the rather different plasma parameters, the overall "plasma dynamics" from the point of view of the Stark broadening effect is rather similar in the two cases, as the estimates of the critical detunings [see Eq. (2)] and a close match between partial ST contributions for the RFD and MFE conditions (Table V) show. Also, both plasmas are weakly coupled. Therefore the Debye screening and other correlation effects are mostly unimportant. Thus let us introduce a dimensionless parameter

$$R = \frac{\ln(w^{MFE}/w^{RFD})}{\ln(N_e^{MFE}/N_e^{RFD})}, \tag{6}$$

where the superscripts indicate the plasma conditions at which the linewidths w are calculated. For a transition broadened by the impact broadening, R would in general depend on T^{MFE} and T^{RFD}. However, for the conditions considered, where an absolute majority of ions as well as a part of electrons are quasistatic, the temperature dependence is rather weak. Thus it is reasonable to expect R to be close to 2/3 (i.e., the exponent in the $w \sim N_e^{2/3}$ scaling in the quasistatic approximation).

Evidently, there are effects that can somewhat complicate the picture, e.g., the quadrupole or the fine-structure corrections, both bearing different importance for the RFD and MFE plasma conditions. In order to avoid this, the same basic approximations should be used when obtaining all the results to be compared thusly. Therefore we took the ST results without the quadrupole corrections, AGT without the dynamical intensities correction, and CSM2 with the fine-structure effects turned off. The results of the comparison are graphically summarized in Fig. 3, covering six high-n Balmer transitions. It is seen that ST and both CSM's agree very well, with the R values confined within a narrow band with an average of about 0.69, which indeed is very close to 2/3. On the other hand, the AGT results occupy a different region. (Here, we assumed the calculated Stark widths in Ref. [6] are given before the convolution with the Doppler broadening; otherwise, the AGT R values would be larger by about 1%.) We also note an irregularity of the AGT R sequence at $n=9$, which should not occur in an analytical theory.

In general, the Stark widths depend rather weakly on the plasma temperature. However, in the case of the MFE conditions, AGT predicts a strong dependence [16] (because of the overestimated ion impact broadening), postulating 7.7 eV instead of 4 eV estimated originally from the Doppler broadening and other considerations [1]. Together with assuming a higher (by about 30%) density, it was claimed to achieve a better agreement with the measured [3] relative linewidths along the series from $n=8$ to $n=11$. We therefore ran the simulations at different temperatures, finding that the widths remained practically constant within the calculation accuracy for temperatures varying between 1 and 8 eV (see Table VI), contrary to the AGT results. We note that there are a few effects that are responsible for the temperature dependence. The sensitivity of the line broadening to the velocities of the perturbers manifests itself in the decrease of the electron impact width for higher temperatures (with the well-known $\sim 1/\sqrt{T}$ asymptotical behavior), and, at the same time, in an increased broadening due to the ion dynamics effect. Therefore these two effects, in addition to being rather weak for

TABLE VI. FWHM (Å) of high-n D Balmer transitions for other MFE conditions.

Line	N_e, cm^{-3}	T, eV	ST[a]	CSM1	CSM2
D_6	5.0×10^{14}	1.0	2.63/2.56	2.53	2.49
	5.0×10^{14}	8.0	2.55/2.41		2.47
D_7	5.0×10^{14}	1.0	3.37/3.17	3.48	3.34
	5.0×10^{14}	8.0	3.05/2.64		3.41
D_8	5.4×10^{14}	4.0	5.20/4.95	5.02	
D_9	5.0×10^{14}	1.0	6.21/5.89		5.80
	5.0×10^{14}	8.0	6.07/5.50		5.81
	5.6×10^{14}	1.0	6.69/6.35	6.78	
	5.6×10^{14}	4.0	6.66/6.19	6.30	
	6.6×10^{14}	4.0	7.43/6.61	7.17	
D_{10}	5.3×10^{14}	4.0	8.47/8.03	8.10	
D_{11}	5.6×10^{14}	4.0	10.7/9.94	10.1	

[a]Values with and without quadrupole corrections.

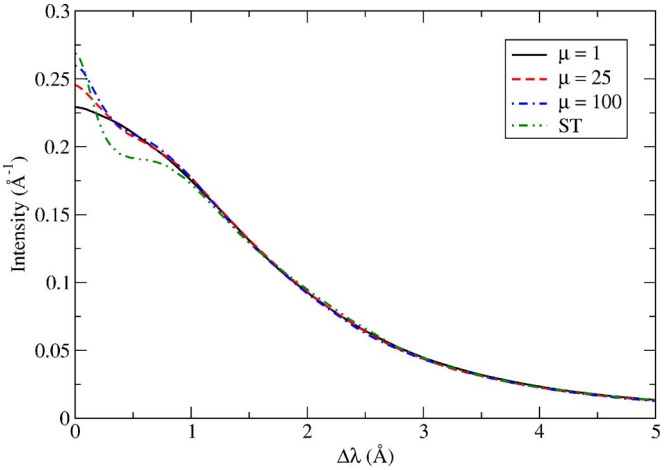

FIG. 4. (Color online) Comparison of ST and CSM2-calculated $n=7$ Balmer profiles, with the reduced ion mass $\mu=1$ (a deuterium radiator in the deuterium plasma) and assumed $\mu=25$ and $\mu=100$. $N_e=5.0\times10^{14}$ cm^{-3}, $T=4.0$ eV. Profiles are area normalized.

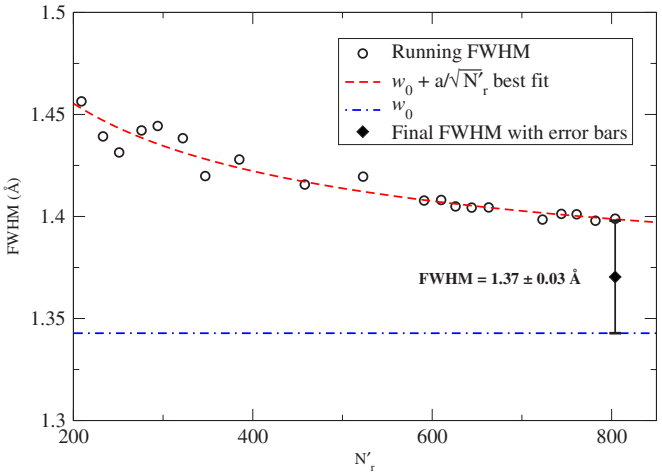

FIG. 5. (Color online) A convergence history of the FWHM of the H_{15} profile under the RFD conditions, calculated using the CSM2 method.

the range of the plasma parameters discussed, cancel each other to a large extent. (The ST calculations, assuming no ion dynamics effects, result in a minor decrease of the linewidths as a function of temperature, as expected). In addition, the Debye screening, which is more effective at lower temperatures, causes a minor decrease in the linewidth as the temperature goes down (e.g., a few percent for T changing from 4 to 1 eV); but for higher temperatures, it becomes practically negligible.

We further note that it is the central (unshifted in the dipole, no-quenching approximation) component of a transition which is most strongly influenced by both the ion dynamics and the electron impact broadening. Therefore transitions with a central component (with an odd upper PQN) have a stronger T dependence than transitions originating from even PQNs. This is confirmed by our ST and CSM results. However, the relative intensity of the central component of high-n transitions is small, decreasing as $\sim 1/n$. Among the spectral lines considered, the Balmer $n=7$ transition has the strongest central component; and thus the effect of the ion dynamics should be maximal. But even for this transition, it is rather weak. In order to confirm this, we also ran the simulations assuming an artificially large reduced ion mass $\mu=25$ and 100. The results are presented in Fig. 4. A minor difference in the line shapes is seen near the center of the profile resulting, e.g., in only a 6% difference between the FWHM values corresponding to $\mu=1$ and 25. With μ increasing, the CSM results approach the ST one (which would correspond to $\mu=\infty$). Finally, we note that the fact that the central component of D_7 is the strongest explains the largest relative value of the quadrupole correction among the lines given in Table III.

VI. CONCLUSIONS

In this paper we have presented numerical simulation results for the typical RFD and MFE experimental parameters by applying full joint electron-ion simulations to Balmer lines with principal quantum number n as high as 15. The ST calculations have been performed as well. Despite the theoretical uncertainty in regard to its estimation of the contribution by strong electron collisions, the ST approach is seen to produce sufficiently accurate results for the range of plasma parameters discussed. At the same time, it has been demonstrated that the impact approximation treatment of broadening by ions, as assumed in AGT, is inappropriate, yielding incorrect density and temperature dependences.

The results presented should be useful for diagnostics of weakly coupled plasmas in a rather broad range of the electron density, 10^{13}–10^{15} cm^{-3}. Comparisons of the calculated spectra with available experimental data in the lower-density region showed a very good agreement. However, accurate measurements of high-n Balmer profiles in the higher-density region are currently lacking. Efforts for obtaining such data, with an independent electron-density determination, are thus highly desirable.

ACKNOWLEDGMENTS

We are indebted to R. D. Bengtson for fruitful discussions and for sharing with us his unpublished experimental data and to R. C. Elton, M. A. Gigosos, M. A. Gonzales, J. Halenka, J. D. Hey, W. Olchawa, J. Seidel, and D. Voslamber for their critical comments. E.S. was partially supported by U.S.-Israel Binational Science Foundation and by Sandia National Laboratories (USA). H.R.G. was partially supported by U.S.-Israel Binational Science Foundation.

APPENDIX: THE ACCURACY OF THE SIMULATIONS

There are several contributions to the total error in the line shape calculations. These can be divided into two groups: the approximations assumed in the corresponding physical model, and the numerical issues pertinent to specific implementations. Among the first, neglecting the electron-radiator quadrupole interactions is probably the most important one (we note that these interactions were included in Ref. [7] and all subsequent ST calculations). This neglect of the quadrupole interaction caused $<1\%$ and $<10\%$ reductions in total

Stark widths for the cases of RFD and MFE plasma conditions, respectively. For the MFE plasma conditions, the present ST results (see Table III), are given with and without the quadrupole corrections. Thus the difference between them can serve as an estimate for inaccuracies introduced into the simulations by omitting the quadrupole interactions. The use of the no-quenching approximation is of less concern. Estimates show that even for the MFE conditions, a contribution of the quadratic Stark effect amounts to about 1% of the total linewidth, and can safely be ignored for the RFD densities.

The numerical uncertainties, in turn, fall into two categories. The first one is the accuracy of the algorithms used, including artifacts inherent to these algorithms, such as the aliasing effects in the discrete Fourier transformation or in the numerical method for solving differential equations. These sources of inaccuracy have been thoroughly evaluated and are believed to contribute only about 1% or less to the total FWHM error bars for all cases considered. For example, in Filon's rule, used for the Fourier transformation in the CSM1 method, the time evolution is solved numerically for $0 \leqslant t \leqslant t_{max}$, with extrapolation to an impact form, if applicable, for longer times. For the RFD H_{10} line, the difference between ignoring the $t > t_{max}$ region in the Fourier integration, i.e., integrating from 0 to t_{max} compared to recognizing an exponential behavior in the autocorrelation function $C(t)$ results in a FWHM of 0.564 Å in the first case, compared to 0.572 Å in the second case. For the RFD H_{11} line, it is only 0.7340 Å, compared to 0.7342 Å.

The second category is specific to CSM calculations, where the motion of the plasma particles is simulated. Evidently, such simulations produce an inherently random perturbing field, and thus averaging the results of many repeated runs is required to obtain an accurate spectrum. The result of such an averaging converges slowly [25], as $\sim 1/\sqrt{N_r'}$ ($N_r' = 1 \cdots N_r$, where N_r is the total number of runs). In the CSM1 calculations, it is verified that enough configurations are used so that the convergence of the autocorrelation function is achieved for the relevant times, i.e., such t that $C(t) \gtrsim 0.1\%$. For longer times, a noise filtering may further be applied during the Fourier transform. To estimate the associated uncertainty in the CSM2 results, we plotted the FWHM value as a function of N_r' during the course of simulations, and then fitted this sequence with a $w_0 + a/\sqrt{N_r'}$ *Ansatz*, using a $\sim N_r'$ weighting function. An average of the best-fit w_0 and the last value of the sequence $w(N_r)$ was taken as the final result, while for the uncertainty, the halfdifference between these values was used.[2] This procedure is demonstrated in Fig. 5, where a convergence history of the FWHM of the H_{15} profile under the RFD conditions is shown. Based on the above considerations, we estimate the total numerical error bars (the algorithm inaccuracies plus the convergence uncertainties) in the CSM2 calculations to be within 3%.

[2]It should be stressed that the main purpose of this FWHM convergence analysis was to obtain a reasonable estimate of the error bars. A choice of the final FWHM is more or less arbitrary as long as it falls within the limits of the error bars; the approach taken here corresponds to assigning equal probabilities to the calculated and the extrapolated values.

[1] B. L. Welch, H. R. Griem, J. Terry, C. Kurz, B. LaBombard, B. Lipschultz, E. Marmar, and G. McCracken, Phys. Plasmas **2**, 4246 (1995).

[2] B. L. Welch *et al.*, in *Spectral Line Shapes*, edited by M. Zoppi and L. Ulivi, AIP Conf. Proc. No. 386 (AIP, Woodbury, NY, 1997), p. 113.

[3] B. L. Welch, H. R. Griem, J. L. Weaver, J. Terry, R. Boivin, B. Lipschultz, D. Lumma, E. S. Marmar, G. McCracken, and J. C. Rost, in *10th Topical Conference on Atomic Processes in Plasmas*, edited by A. Osterheld and W. H. Goldstein, AIP Conf. Proc. No. 381 (AIP, Woodbury, NY, 1996), p. 159.

[4] R. Ellis, A. Case, R. C. Elton, J. Ghosh, H. R. Griem, A. Hassam, R. Lunsford, S. Messer, and C. Teodorescu, Phys. Plasmas **12**, 055704 (2005).

[5] R. D. Bengtson, J. D. Tannich, and P. C. Kepple, Phys. Rev. A **1**, 532 (1970).

[6] E. Oks, R. D. Bengtson, and J. Touma, Contrib. Plasma Phys. **40**, 158 (2000).

[7] P. C. Kepple and H. R. Griem, Phys. Rev. **173**, 317 (1968).

[8] G. V. Sholin, A. V. Demura, and V. S. Lisitsa, Zh. Eksp. Teor. Fiz. **64**, 2097 (1973) [Sov. Phys. JETP **37**, 1057 (1973)].

[9] H. R. Griem, *Spectral Line Broadening by Plasmas* (Academic, New York, 1974).

[10] Y. Ispolatov and E. Oks, J. Quant. Spectrosc. Radiat. Transf. **51**, 129 (1994).

[11] J. Touma, E. Oks, S. Alexiou, and A. Derevianko, J. Quant. Spectrosc. Radiat. Transf. **65**, 543 (2000).

[12] R. Stamm and D. Voslamber, J. Quant. Spectrosc. Radiat. Transf. **22**, 599 (1979).

[13] M. A. Gigosos and V. Cardeñoso, J. Phys. B **20**, 6065 (1987).

[14] J. Holtsmark, Ann. Phys. **58**, 577 (1919).

[15] H. A. Lorentz, Proc. R. Acad. Sci. Amsterdam **8**, 591 (1906).

[16] E. Oks, Phys. Rev. E **60**, R2480 (1999).

[17] C. Stehle, Astron. Astrophys. **305**, 677 (1996).

[18] V. Kogan, in *Plasma Physics and the Problems of Controlled Thermonuclear Reactions*, edited by M. A. Leontovich (Pergamon, Oxford, 1960), Vol. IV, p. 305.

[19] G. C. Hegerfeldt and V. Kesting, Phys. Rev. A **37**, 1488 (1988).

[20] J. Seidel, in *Spectral Line Shapes*, edited by L. Frommhold and J. Keto, AIP Conf. Proc. No. 216 (AIP, New York, 1990), pp. 98–99.

[21] J. Seidel, Verh. Dtsch. Phys. Ges. **25**, 372 (1990).

[22] S. Alexiou, Phys. Rev. E **71**, 066403 (2005).

[23] S. Alexiou, J. Quant. Spectrosc. Radiat. Transf. **69**, 667 (2001).

[24] S. Alexiou, J. Quant. Spectrosc. Radiat. Transf. **81**, 13 (2003).

[25] E. Stambulchik and Y. Maron, J. Quant. Spectrosc. Radiat.

Transf. **99**, 730 (2006).
[26] J. Halenka and W. Olchawa, J. Quant. Spectrosc. Radiat. Transf. **56**, 17 (1996).
[27] R. D. Bengtson (private communication).
[28] H. R. Griem, J. Halenka, and W. Olchawa, J. Phys. B **38**, 975 (2005).
[29] S. Alexiou, H. R. Griem, J. Halenka, and W. Olchawa, J. Quant. Spectrosc. Radiat. Transf. **99**, 238 (2006).
[30] M. L. Strekalov and A. I. Burshtein, Zh. Eksp. Teor. Fiz. **61**, 101 (1971) [Sov. Phys. JETP **34**, 53 (1972)].
[31] E. Oks, J. Quant. Spectrosc. Radiat. Transf. **99**, 247 (2006).
[32] S. Flih, E. Oks, and Y. Vitel, J. Phys. B **36**, 283 (2003).
[33] S. Alexiou and A. Poquérusse, Phys. Rev. E **72**, 046404 (2005).
[34] H. A. Bethe and E. E. Salpeter, *Quantum Mechanics of One- and Two-Electron Atoms* (Plenum, New York, 1977).
[35] J. D. Hey, M. Korten, Y. T. Lie, A. Pospieszczyk, D. Rusbüldt, B. Schweer, B. Unterberg, J. Wienbeck, and E. Hintz, Contrib. Plasma Phys. **36**, 583 (1996).
[36] R. M. Pengelly and M. J. Seaton, Mon. Not. R. Astron. Soc. **127**, 165 (1964).
[37] R. D. Bengtson and G. R. Chester, Phys. Rev. A **13**, 1762 (1976).